J. Sci. I. R. Iran

Vol. 6 No. 3
Summer 1995

AXIAL FLOW OF CASSON PLASTIC MODEL IN ANNULUS WITH A ROTATING INNER CYLINDER

S.H. Javadpour and R. Farrahi Moghaddam

Department of Mathematics, University of Kerman, Kerman, Islamic Republic of Iran.

Abstract

This paper describes a solution for the flow of a viscoplastic material in a circular Couette drive with an imposed axial flow, sometimes called a helical flow. The problem is interesting because for a non-Newtonian fluid the circular Couette flow and pressure driven axial flow are coupled, whereas for a Newtonian fluid these flows are uncoupled. In the last three decades, theoretical analysis of helical flow of non-Newtonian fluids has been attempted by many authors. The solutions have been obtained in terms of several variables including impressed axial pressure gradient in the annulus and the rheological model parameters. The fluid models are an idealization of a certain class of complex fluids which show yielding behavior when an applied shear stress exceeds a certain critical value, called the yield value. We have considered two different conditions. These arise from the fact that when the shear stress is below the yield value, at some point in the annulus region the fluid will behave like a solid, whereas when the shear stress is above the yield value at all points within the annulus there is no solid (plug) region. We obtain a solution for the axial flow of viscoplastic material between two concentric cylinders. The inner cylinder is assumed to rotate about its axis with angular speed Ω, while the outer cylinder is stationary. Rotation of the inner cylinder drives the tangential flow of the fluid contained in the gap. We present the results in the form of relation between dimensionless parameters involving the moment acting on inner cylinder, the volumetric flow rate, the fluid properties, and the dimensions of the annulus. By numerical integration, prediction is made of axial velocity profile, azimutal velocity profile, and axial and radial pressure gradient profiles in the annular region. These profiles are found to be affected by axial flow as well as rotation velocity.

Introduction

Treatment of helical flow was first considered by Rivlin and Ericksen [1,2]. Rivlin presented his results in terms of eight material functions, however Coleman and Noll [3,4] showed that only three are necessary. Fredrickson [5] used the constitutive equation developed by Rivlin and introduced an arbitrary function which turned out to be simply the shear dependent viscosity. Dierckes and Schowalter [6] presented an analytic solution for a power law fluid in a system with the outer cylinder rotating. Rea and Schowalter [7] experimentally measured the velocity

Keywords: Helical flow: Casson plastic model; Rheology

profile of a power law fluid in a helical flow system and compared their findings with predictions made from tube viscometer data.

Tanner [8] presented the theory of helical flow as applied to a model by Oldroyd [9], along with some experimental results. Savins and Wallick [10] made quantitative predictions to show how the axial discharge rate and pressure gradient, as well as angular velocity and torque, become coupled when a fluid exhibiting a shear-dependent viscosity behaviour is subjected to a helical flow field.

Bird *et al.* [11] produced an analytical solution to the equations for helical flow in a very thin annulus for power law fluids, for a power law index n= 1/3. Huilgol [12] proposed a trial and error method to solve the helical flow problem for general fluids in terms of four parameters, including one related to the axial pressure gradient. Detailed numerical analysis of the helical flow of power law fluids for any cylinder dimensions, and experimental verification was carried out by Sestak *et al.* [13]. Bhattacharya *et al.* [14] solved the problem of axial flow in a rotational rheometer for power law flows. In their final equations, the axial pressure gradient term was eliminated, thereby reducing the number of variable parameters to three. Javadpour and Bhattacharya [15, 16] solved the problem of axial flow in a rotational rheometer in a series of papers for Bingham plastic and Herschel-Bulkley models. They were able to obtain the shear rate-shear stress relation and viscosity distribution for different values of the flow rate, torque and yield stress.

Javadpour [17] presented the viscosity distribution and velocity profile for the helical flow of a Herschel-Bulkley fluid, in terms of dimensionless variables for the volumetric flow rate, moment acting on inner cylinder and fluid properties.

The main goal of this paper is to present a detailed numerical solution to the helical flow of a viscoplastic material as Casson plastic model [18], for any cylinder dimensions. We consider three distinct situations for different values of dimensionless parameters for the two cases where a plug region does or does not exist in the gap.

Formulation

We consider the fluid to be contained between two coaxial cylinders of radii R_1 and R_2 where ($R_1<R_2$). A helical flow pattern was generated by pumping the solution through an annular space, while rotating the inner cylinder with angular velocity Ω.

We use cylindrical coordinates

$$x^1= r,\ x^2= \theta,\ x^3= z \qquad (1)$$

The velocity field of the fluid in this coordinate system is

$$\underline{v}= (v_r=0\ ,\ v_\theta=r\omega(r)\ ,\ v_z=v(r)) \qquad (2)$$

which automatically satisfies the equation of continuity.

We consider the Casson equation. The relation between shear stress and shear rate is given by,

$$\begin{cases} \tau_{ij}=\eta(\dot\gamma)\dot\gamma_{ij},\ \eta(\dot\gamma)=\tau/\dot\gamma, \\ \tau^{1/2}=\tau_0^{1/2}+(\mu_0\dot\gamma)^{1/2} \quad \text{if} \quad |\tau|\geq\tau_0 \\ \dot\gamma=0 \qquad\qquad \text{if} \quad |\tau|\leq\tau_0 \end{cases} \qquad (3)$$

where τ_0 is the yield stress; μ_0 is the limiting viscosity and $\dot\gamma$ is given by

$$\dot\gamma=\sqrt{(r\omega'(r))^2+(v'(r))^2}, \qquad (4)$$

where $\dot\gamma$ is defined as total shear rate and prime denotes the derivative with respect to r.

The nonslip boundary condition at the inner (R_1) and outer (R_2) cylinder are

$$v_z(R_1)= v_z(R_2)= 0, \qquad (5)$$

$$v_\theta(R_1)= R_1\Omega,\ v_\theta(R_2)= 0$$

If we express the gravitational force in terms of a scalar potential Ψ by

$$g= -\nabla\Psi \qquad (6)$$

and define

$$\Phi=P+\rho\Psi \qquad (7)$$

where P is the fluid pressure and ρ is the fluid density (constant), the equations of motion take the form

$$\frac{1}{r}\frac{d}{dr}(r\tau_{rr}) - \frac{1}{r}\tau_{\theta\theta} - \frac{\partial\Phi}{\partial r} = -\rho r\omega^2 \qquad (8)$$

$$\frac{1}{r}\frac{d}{dr}(r\tau_{rz}) - \frac{\partial\Phi}{\partial z} = 0 \qquad (9)$$

$$\frac{1}{r}\frac{d}{dr}(r^2\tau_{r\theta}) = 0 \qquad (10)$$

The nonzero components of the total stress tensor are

$$\tau_{r\theta}=r\omega'(r)\,\eta(\Pi),\ \tau_{rz}=v'(r)\,\eta(\Pi) \qquad (11)$$

where Π is the second invariant of the strain rate tensor.

It can be shown from equation (10) that the stress field, regardless of the fluid rheology, is given by

$$\tau_{r\theta} = -\frac{M}{2\pi r^2} \qquad (12)$$

where $M/2\pi$ is the moment per unit length in the axial direction to maintain the rotating flow. It is worth noting that because the inner cylinder rotates and the outer one is stationary $\omega'(r)<0$ and hence $\tau_{r\theta}$ is negative.

The physical variables can be written in nondimensional form through the substitutions

$$r^* = \frac{r}{R_2},\ z^* = \frac{z}{R_2},\ v_\theta^* = \frac{r\omega(r)}{R_1\Omega},\ v_z^* = \frac{v(r)}{R_1\Omega},$$

$$\omega^* = \frac{R_2}{R_1\Omega}\omega,\ \dot\gamma^* = \frac{R_2}{R_1\Omega}\dot\gamma,\ \tau_{ij}^* = \frac{\tau_{ij}}{\mu_0 R_1\Omega/R_2} \qquad (13)$$

and

$$Q^* = \frac{Q}{\pi\left(R_2^2 - R_1^2\right)R_1\Omega},\ M^* = \frac{M}{\mu_0 R_1 R_2 \Omega},$$

$$\Phi^* = \frac{R_2\Phi}{R_1\Omega\,\mu_0}$$

and $\tau_0^* = \frac{R_2}{\mu_0 R_1\,\Omega}\tau_0$ is called Casson number.

The dimensionless form of the equations of motion are

$$\frac{\partial}{\partial r^*}\Phi^* = R_{eq.}\, r^*\omega^{*2} \qquad (14)$$

$$\frac{1}{r^*}\frac{d}{dr^*}\left(r^*\tau_{r^*z^*}^*\right) - \frac{\partial\Phi^*}{\partial z^*} = 0 \qquad (15)$$

$$\frac{1}{r^*}\frac{d}{dr^*}\left(r^{*2}\tau_{r^*\theta}^*\right) = 0 \qquad (16)$$

where the equivalent Reynold number is

$$R_{eq.} = \rho R_2(R_1\,\Omega)/\mu_0$$

From equation (14), using equation (15) and the fact of depending the stress only on r that result from equation (2) and postulate for a simple fluid, we obtain

$$\Phi^* = R_{eq.}\int_a^1 r^*\omega^{*2}(r^*)\,dr^* + 2\alpha z^* \qquad (17)$$

where 2α is effective axial pressure gradient and is constant.

The nondimensional form of equation of state can be written as

$$\tau^{*1/2} = \tau_0^{*1/2} + \dot\gamma^{*1/2} \qquad (18)$$

The boundary conditions become

$$v_{z^*}^*(a) = v_{z^*}^*(1) = 0\ ,\ v_\theta^*(a) = 1 \text{ and } v_\theta^*(1) = 0 \qquad (19)$$

where $a = R_1/R_2$, τ^* and $\dot\gamma^*$ are defined by (13).

Solving equations (15-16), we obtain the stress components as

$$\tau_{r^*z^*}^* = \alpha r^* + \beta/r^*\ ,\ \tau_{r^*\theta}^* = -M^*/(2\pi r^{*2}) \qquad (20)$$

For helical flow of a fluid for $|\tau| \geq \tau_0$, using equations (11) and (20) we obtain

$$\eta^*(\dot\gamma^*)\, r^*\omega'^*(r^*) = -M^*/2\pi r^{*2} \qquad (21)$$

$$\eta^*(\dot\gamma^*)\, v'(r^*) = \alpha r^* + \beta/r^* \qquad (22)$$

Using equation of state (18) and defining the total shear stress as $\tau^* = \sqrt{\tau_{r^*z^*}^{*2} + \tau_{r^*\theta}^{*2}}$, from equations (4) and (21-22) we obtain

$$\dot\gamma^* = \left[\sqrt[4]{\left(M^*/2\pi r^{*2}\right)^2 + \left(\alpha r^* + \beta/r^*\right)^2} - \tau_0^{*1/2}\right]^2 \qquad (23)$$

and

$$\omega'^*(r^*) = -\left(\frac{M^*}{2\pi r^{*3}}\right)\times$$

$$\frac{\left[\sqrt{\left(M^*/2\pi r^{*2}\right)^2 + \left(\alpha r^* + \beta/r^*\right)^2} - \tau_0^{*1/2}\right]^2}{\sqrt{\left(M^*/2\pi r^{*2}\right)^2 + \left(\alpha r^* + \beta/r^*\right)^2}} \qquad (24)$$

$$v'^*(r^*) = \left(\alpha r^* + \frac{\beta}{r^*}\right)\times$$

$$\frac{\left[\sqrt{\left(M^*/2\pi r^{*2}\right)^2+\left(\alpha r^*+\beta/r^*\right)^2}-\tau_0^{*1/2}\right]^2}{\sqrt{\left(M^*/2\pi r^{*2}\right)^2+\left(\alpha r^*+\beta/r^*\right)^2}} \tag{25}$$

Note that when $\tau_0 = 0$, then $v'^*(r^*)=\left(\alpha r^* + \frac{\beta}{r^*}\right)$ which is in its Newtonian form.

We now have to consider three distinct situations for each value of the Casson number τ_0^* by choosing the volumetric flow rate Q^* as a constant, while M^* changes, and vice versa.

Case I

When $|\tau| > \tau_0^*$, everywhere in the annulus i.e. shearing stress is above the yield value at all points within the gap, then integrating ω'^* subject to the boundary conditions gives

$$\int_a^1 \omega'^*(r^*)\,dr^* = \Omega^* \tag{26}$$

and integrating (25) subject to conditions (19) gives

$$G_1(\alpha,\beta)=\int_a^1 v'^*(r^*)\,dr^*=0 \tag{27}$$

Using the fact that the axial flow rate at any cross-section of the annulus is constant, we obtain

$$G_2(\alpha,\beta)=\int_a^1 r^{*2}v'^*(r^*)\,dr^* + Q^*(1-a^2)=0 \tag{28}$$

Case II

We have $\tau^*(r_3)=\tau_0^*$ where $a<r_3<1$. Therefore, particles in the fluids occupying the region between $r_3 \le r^* \le 1$ have zero velocity, material near the outer cylinder will behave like a solid with $\dot{\gamma}=0$, and flow occurs only for values of r^* such that $a<r^*<r_3$. Thus we write

$$\int_a^{r_3} \omega'^*(r^*)\,dr^*=\Omega^* \tag{29}$$

$$G_1(\alpha,\beta)=\int_a^{r_3} v'^*(r^*)\,dr^*=0 \tag{30}$$

$$G_2(\alpha,\beta)=\int_a^{r_3} r^{*2}\,v'^*(r^*)\,dr^* + Q^*(1-a^2)=0 \tag{31}$$

Case III

If there are two values such as r_3 and r_4 between a and 1 in which $\tau^*(r_3)=\tau^*(r_4)=\tau_0^*$, then particles in the fluids occupying the region between $r_3 \le r^* \le r_4$ have constant velocity and the material in this region moves as a solid plug, in this case we have,

$$\left(\int_a^{r_3}+\int_{r_4}^1\right)\omega'^*(r^*)\,dr^*=\Omega^* \tag{32}$$

$$G_1(\alpha,\beta)=\left(\int_a^{r_3}+\int_{r_4}^1\right)v'^*(r^*)\,dr^*=0 \tag{33}$$

$$G_2(\alpha,\beta)=\left(\int_a^{r_3}+\int_{r_4}^1\right)r^{*2}v'^*(r^*)\,dr^* + Q^*(1-a^2)=0 \tag{34}$$

Numerical Techniques

By the numerical integration of the equations $G_1(\alpha,\beta)=G_2(\alpha,\beta)=0$ with the use of Simpson's rule and the aid of the Microsoft Excel Solver which uses the GRG2 nonlinear optimization [19], we found α and β for each case.

The values of α and β may be applied to calculate the components of velocity and the magnitude of velocity |v| expressed as equal to $\sqrt{v_z^{*2}+v_\theta^{*2}}$ at the different points in the annular region. Viscosity may be obtained as total shear stress divided by the total shear rate.

Results and Discussion

We have studied the helical flow of a viscoplastic material as Casson plastic model between a coaxial annular region. The effect of volumetric flow rate as well as rotation velocity on the axial velocity and the azimutal velocity profiles within the annulus is predicted. Comparisons were made for decreasing moment acting on inner cylinder for two values of volumetric flow rate.

We carried out studies of the problem when at some points within the annulus the value of shearing stresses goes below the yield value. In this region, the fluid will

behave like a solid. We find that there is an interesting structural change in the velocity patterns with changes in the volumetric flow rate and rotating velocity which was not considered in the earlier studies.

Total shear stress and total shear rate relation for a Casson model is presented in Figure 1. The full line represents the graph of the nondimensional form of the equation of state and the dotted line represents the different volumetric flow rates and shows that the axial flow rate did not have any effect on the flow behaviour curve. Similar behaviour was observed for Herschel-Bulkley and Bingham plastic fluids [15, 16].

The velocity profile in a helical flow will be dependent on the magnitude of the azimutal component of velocity imparted by the rotating cylinder and axial velocity component due to the imposed axial flow. In Figure 2, the axial velocity component has been estimated for a constant flow rate corresponding to various moments acting on the inner cylinder.

It should be pointed out that at low values of flow rate and decreasing moment acting on the inner cylinder three cases will arise. In case II and III we can see a solid plug. In case II particles near the outer cylinder have zero velocity, while in case III, particles in the middle of the gap have constant velocity, i.e. the material in this region moves as a solid plug. The azimutal velocity profile for the same values as Figure 2 is presented in Figure 3. The magnitude of velocity |v| expressed as equal to $\sqrt{v_z^{*2} + v_\theta^{*2}}$ is plotted against the radial position in Figure 4.

Comparisons were made for increasing flow rate. Inspection of Figures 5,6, and 7 indicates that only cases I and III will happen with increasing flow rate. The effect of increasing Casson number is shown in Figures 8, 9 and 10.

Theoretical prediction of viscosity profile in the annular gap is presented in Figure 11. Viscosity goes through a peak in the annular gap. The location of this peak is dependent on the value of M. In case II at one point we have $\tau = \tau_0$ but in case III there are two points of discontinuity for viscosity profile.

In Figure 12, effective pressure profile for a constant flow rate has been presented. In Figure 13, effective pressure gradient has been shown versus volumetric flow rate, for two values of moment acting on the inner cylinder. For a constant value of M^*, α increases with Q^* and has nonlinear behaviour for low values of Q^*, whereas for a Newtonian fluid α is proportional to Q^*. Furthermore, α decreases as M^* increases for small values of Q^*. Effective radial pressure gradient profile for the same values as in Figure 12 is presented in Figure 14. As M^* decreases, radial pressure gradient decreases near the inner cylinder.

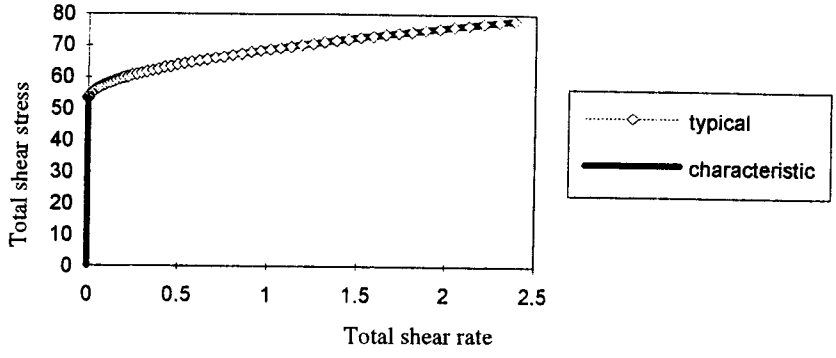

Figure 1. Total shear stress-total shear rate relation

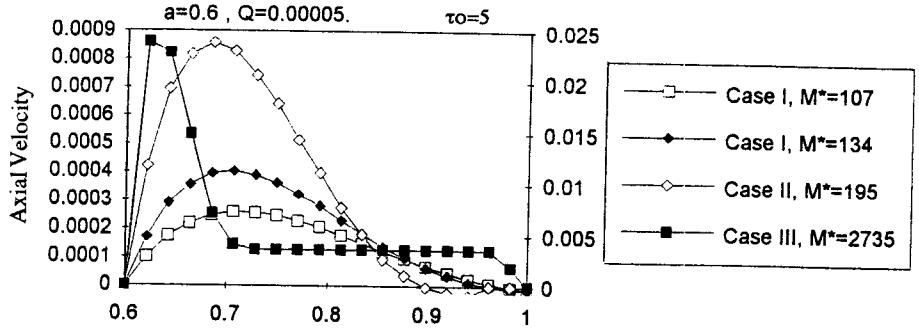

Figure 2. Axial velocity profile for a constant flow rate

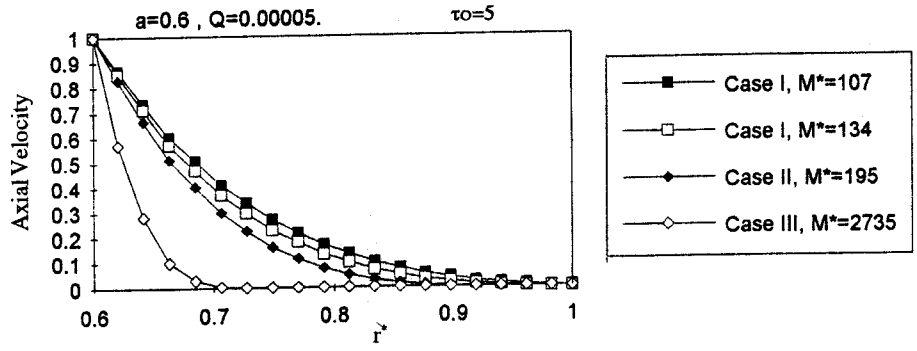

Figure 3. Azimutal velocity profile for a constant flow rate

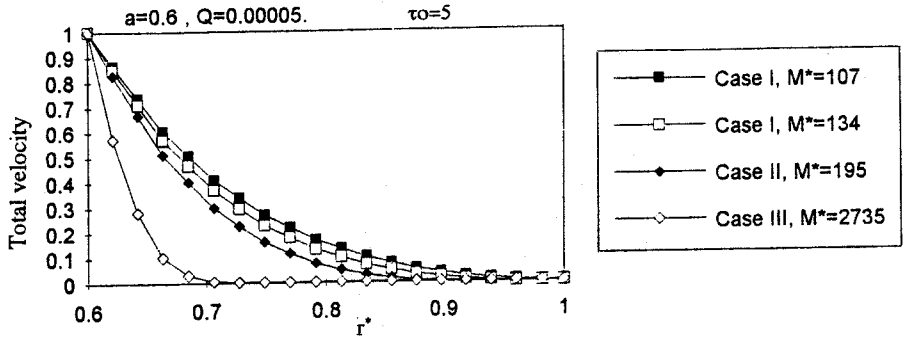

Figure 4. Total velocity profile for a constant flow rate

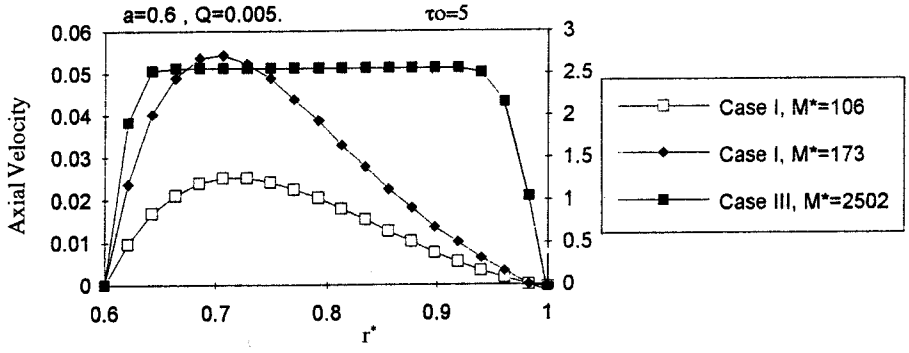

Figure 5. Axial velocity profile for a constant flow rate

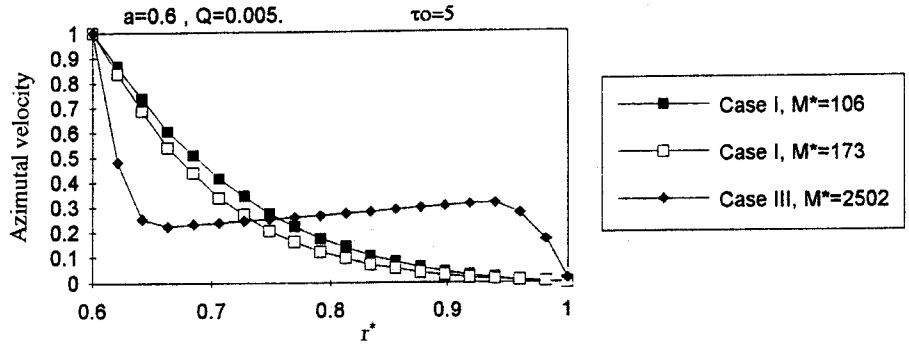

Figure 6. Azimutal velocity profile for a constant flow rate

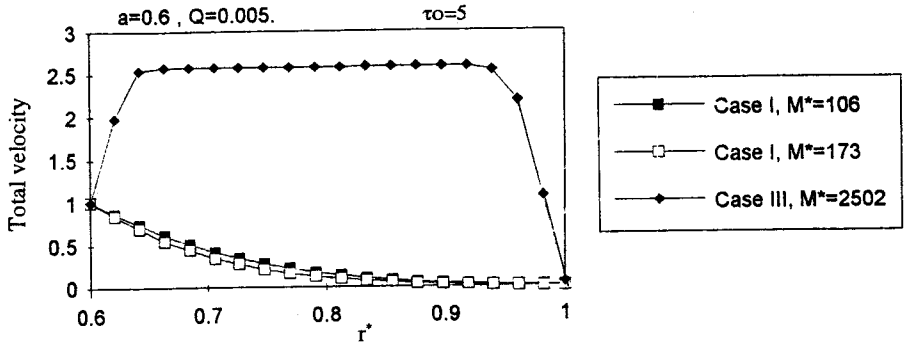

Figure 7. Total velocity profile for a constant flow rate

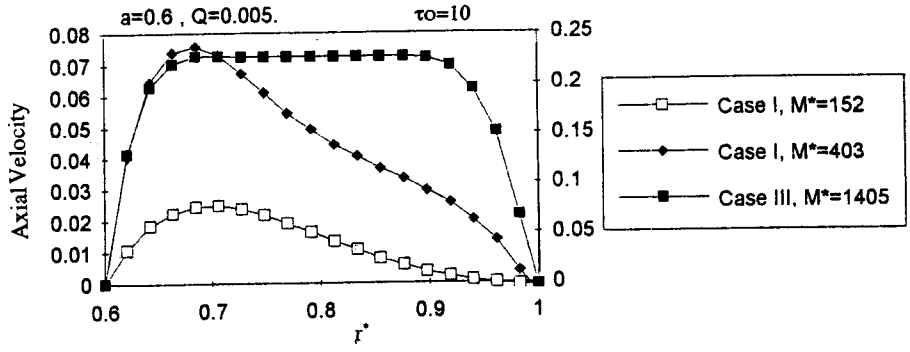

Figure 8. Axial velocity profile for a constant flow rate

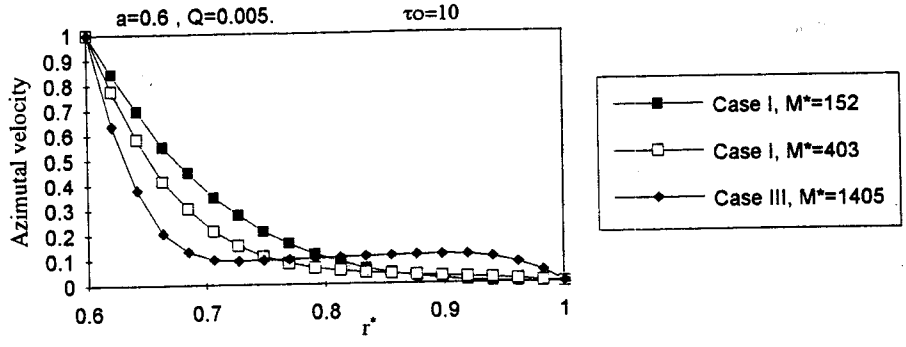

Figure 9. Azimutal velocity profile for a constant flow rate

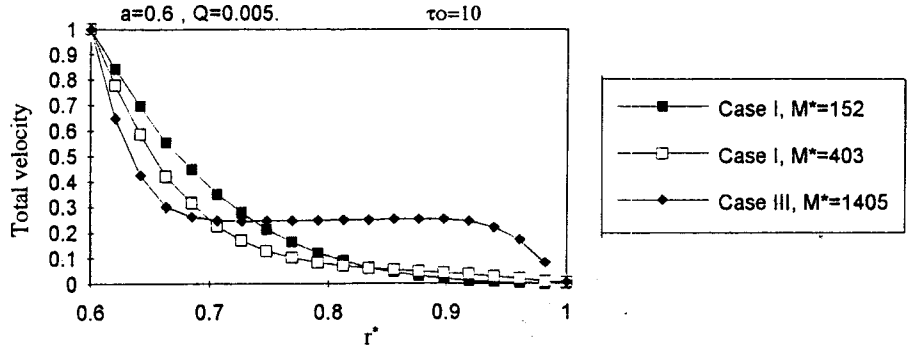

Figure 10. Total velocity profile for a constant flow rate

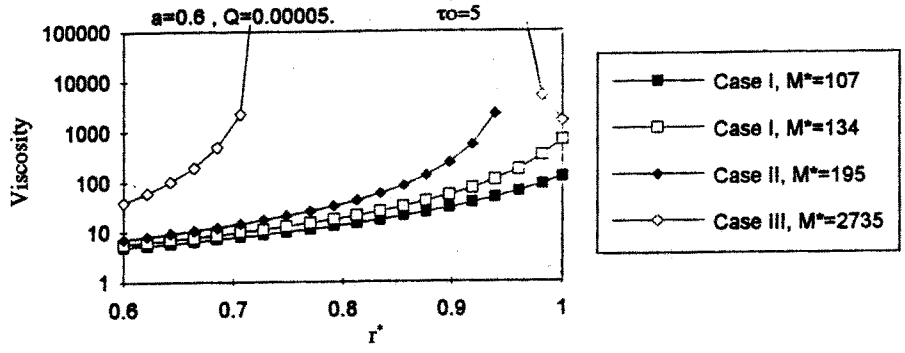

Figure 11. Viscosity profile for a constant flow rate

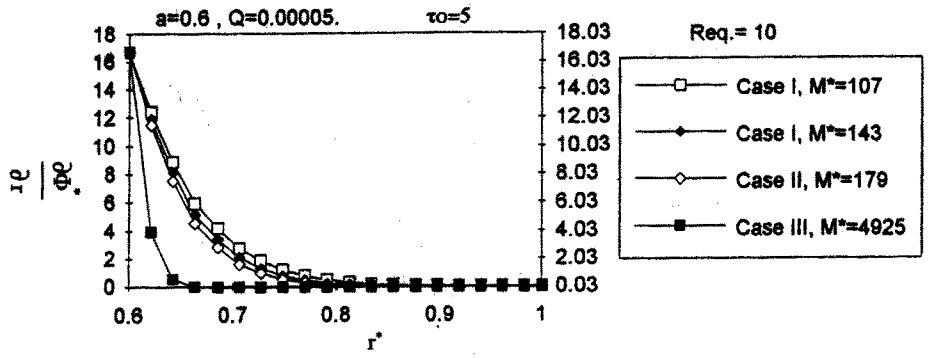

Figure 12. Effective radial pressure gradient profile for a constant flow rate

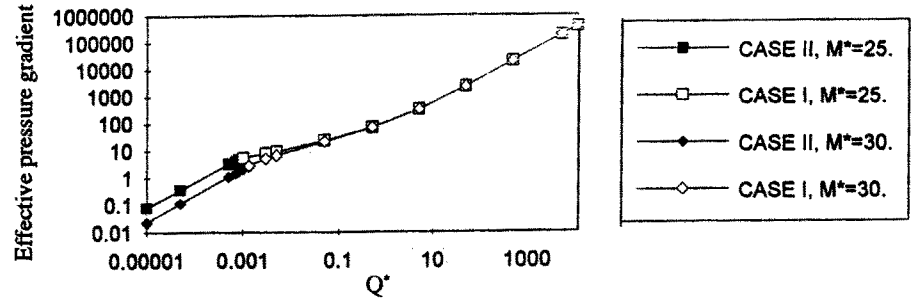

Figure 13. Effective axial pressure gradient versus flow rate

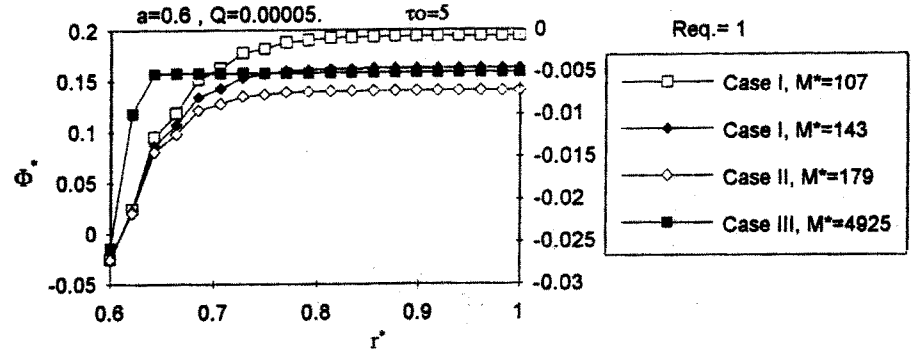

Figure 14. Effective pressure profile for a constant flow rate

Acknowledgements

The authors would like to express their gratitude to the referees for their valuable comments and careful reading of the paper. The financial assistance given by the Mahani Mathematical Research Center of the University of Kerman is gratefully acknowledged.

References

1. Rivlin, R.S., Ericksen, J.F. *J. Rational Mech. Anal.*, **4**, 323, (1955).
2. Rivlin, R.S. *Ibid.*, **5**, 179, (1956).
3. Coleman, B.D. and Noll, W. *Arch. Rational Mech. Anal.*, **3**, 289, (1959).
4. Coleman, B.D. and Noll, W. *J. Applied Phys.*, **30**, 10, 1508, (1959).
5. Fredrickson, A.G. *Chem. Eng. Sci.*, **11**, 252, (1960).
6. Dierckes, A.C. and Schowalter, W. *Ind. Eng. Chem. Fund.*, **5**, 263, (1966).
7. Rea, D.R. and Schowalter, W. *Trans. Soc. Rheol.*, **11**, 125, (1967).
8. Tanner, R.I. *Rheo. Acta.*, **3**, Part I, 21, Part II, 26, (1963).
9. Oldroyd, J.G. *Proc. Roy. Soc.*, **A 245**, 278, (1958).
10. Savins, J.G. and Wallick, G.C. *A.I.Ch.E.J.*, **12**, 357, (1966).
11. Bird, R.B., Armstrong, R.C. and Hassager O. *Dynamics of polymeric liquids*, Vol. 1, John Wiley & Sons (1987).
12. Huilgol, R.R. 5th National Conf. Rheo. Melbourne, 43, (1990).
13. Sestak, J., Houska, M., Zity, R. and Dostal, M., 3rd European Conf. Rheo., 473, (1990).
14. Bhattacharya, S.N., Chryss, A., Connell, H.J. and Shepherd, J.J. 5th National Conf. Rheo. Melbourne, 15, (1990).
15. Javadpour S.H., Bhattacharya, S.N. *J. Sci. I.R. Iran*, **2**, 151, (1991).
16. Javadpour, S.H., Bhattacharya, S.N. *J. Sci. I.R. Iran*, **3**, 70, (1992).
17. Javadpour, S.H. *Inter. J. of Eng. IUST*, **4**, 37, (1993).
18. Casson, N. In *Rheology of disperse system*, (ed. C.C. Mill) p. 84, Pergamon, (1959).
19. Lasdon, L. and Allan, W. *The GRG2 nonlinear optimization code*, The Microsoft Excel Solver Program. Frontline Systems, Inc. (1990).